Article published in Physics and Chemistry of Minerals, 2002, Volume 29, 477-484

The final publication is available at Springer via http://dx.doi.org/10.1007/s00269-002-0259-1.

Structural characterization of high pressure C - $Na_2Si_2O_5$ by single crystal diffraction and ^{29}Si MAS NMR

S. Rakić[1], V. Kahlenberg[1], C. Weidenthaler[2], B. Zibrowius[2]

[1]Fachbereich Geowissenschaften (Kristallographie), Universität Bremen, Klagenfurter Str., D - 28359 Bremen, Germany

[2]Max-Planck-Institut für Kohlenforschung, Kaiser-Wilhelm-Platz 1, D - 45470 Mülheim an der Ruhr, Germany

Post-print version

Abstract

Single crystals of C-$Na_2Si_2O_5$ have been synthesized from the hydrothermal recrystallization of a glass. The title compound is monoclinic, space group $P2_1/c$ with Z = 8 and unit cell parameters a = 4.8521(4)Å, b = 23.9793(16)Å, c = 8.1410(6)Å, β = 90.15(1)°, V = 947.2(2)Å^3. The structure has been determined by direct methods and belongs to the group of phyllosilicates. It is based on layers of tetrahedra with elliptically six-membered rings in chair conformation. The sequence of directedness within a single ring is UDUDUD. The sheets are parallel to (010) with linking sodium cations in five- and six-fold coordination. Concerning the shape and the conformation of the rings C-$Na_2Si_2O_5$ is closely related to β-$Na_2Si_2O_5$. However, both structures differ in the stacking sequences of the layers. A possible explanation for the frequently observed polysynthetic twinning of phase C is presented. In the ^{29}Si MASNMR spectrum of C-$Na_2Si_2O_5$ four well-resolved lines of equal intensity are observed at -86.0, -86.3, -87.4, and -88.2 ppm. The narrow range of isotropic chemical shifts reflects the great similarity of the environments of the different Si sites. This lack of pronounced differences in geometry renders a reliable assignment of the resonance lines to the individual sites on the basis of known empiric correlations between and geometrical features impossible.

Key Words : single layer silicate, sodium disilicate, C-$Na_2Si_2O_5$, single crystal structure analysis, twinning, phyllosilicate, ^{29}Si MAS NMR

Post-print version

Introduction

Sodium disilicates are of interest in mineralogy and solid state chemistry as well. Melts with composition $Na_2Si_2O_5$, for example, have been used by geoscientists as models for silicate melt phases which are the essential components of nearly all igneous processes (Kanzaki *et al*. 1998; Maekawa *et al*. 1997). Crystalline sodium disilicates and especially δ-$Na_2Si_2O_5$ have been studied because of their interesting high ion exchange capacity and selectivity (Wolf and Schwieger, 1979). A review of the industrial applications can be found in the paper of Rieck (1996). Furthermore, a complex polymorphism with at least eight different stable and metastable phases has been reported for $Na_2Si_2O_5$ as a function of temperature, pressure and synthesis conditions (Willgallis and Range, 1963; Williamson and Glasser, 1966; Hoffmann and Scheel, 1969). However, the crystal structures of several of these modifications remain to be solved.

The phase equilibrium diagram for the system $Na_2Si_2O_5$ in the range between room pressure and 400 bars has been investigated by Williamson and Glasser (1966). Three thermodynamically stable phases have been observed : α-$Na_2Si_2O_5$, β-$Na_2Si_2O_5$ and another high pressure polymorph designated ‘phase C‘. The triple point between the three phases is located at about 715°C and 90 bars. A preliminary investigation of phase C indicated monoclinic symmetry and a pseudo-orthorhombic metric (a = 8.12Å, b = 23.7 Å, c = 4.85 Å, β = 90°). However, no detailed structural characterization was performed. The results of Williamson and Glasser (1966) concerning the existence of a sodium disilicate modification with a stability range starting at slightly elevated pressures were confirmed by Jacobsen (1991). The phase relations in the $Na_2Si_2O_5$ system especially at higher pressures have been studied by Kanzaki *et al.* (1998). According to their results the stability field of phase C extends to at least 25 kbar (at

Post-print version

900°C). At pressures of about 50-60 kbar a new phase (ε- $Na_2Si_2O_5$) appears.

In the course of an ongoing project on the crystal chemistry and the phase transitions in sodium and potassium disilicates we obtained single-crystals of phase C. The aim of the present work is to provide a description of the crystal structure of this compound and to show the relationships with known silicate structures. Preliminary results obtained by ^{29}Si MASNMR spectroscopy are also included.

Experimental Details

The single crystals in this study were synthesized from a glass of $Na_2Si_2O_5$ composition. The glass was prepared by fusing a stoichiometric mixture of Na_2CO_3 (Fluka, 99%) and SiO_2 (fine grained quartz powder) in a covered platinum crucible at 1000°C for 1 h and quenching in air. The product was crushed and then ground in acetone. The melting process was repeated for two times in order to increase the homogeniety of the glass. Approximately 0.19 g of the glass and 2 ml of H_2O were loaded and sealed in a gold capsule (about 3 mm in diameter and 30 mm in height). The hydrothermal experiment was performed in an externally heated Morey-type autoclave. The sample was taken at room temperature to a pressure of 1 kbar, and subsequently taken to a temperature of 750°C. The run duration at the final temperature was 24 h. After quenching, the recovered sample consisting of transparent, colorless, platy crystals up to 0.3 mm in diameter was examined using a petrographic microscope. Almost all crystals showed a polysynthetic twinning.

For the structural investigations one of the rare untwinned crystals (0.24 x 0.12 x 0.006 mm in size) was selected. A total of 6124 reflections up to 24.2° θ were collected at 20°C on a Stoe imaging plate detector system IPDS (graphite-monochromatized MoK_α radiation). Table 1 contains a summary of the conditions

Post-print version

for the data collection and of the subsequent structure refinement parameters. All the data were numerically corrected for absorption by use of 9 indexed external faces. Data reduction including intensity integration, background corrections, Lorentz and polarisation correction was performed with the Stoe XRED program package.

Table 1

The diffraction symmetry of the crystal was consistent with Laue group 2/*m*. The systematic reflection conditions *h0l*: *l* = 2*n* ; 0*k*0: *k* = 2*n* unambiguously indicated the space group was $P2_1/c$ (No. 14). The structure was solved by direct methods with the program SIR92 (Altomare *et al.*, 1992) using a multisolution process. The phase set with the maximum combined figure of merit resulted in an E-map, the most intense peaks of which could be interpreted as a layer structure. Least squares refinements were performed with the program SHELXL-93 (Sheldrick 1993). Neutral-atom scattering factors and anomalous-dispersion corrections were taken from the *International Tables for X-ray crystallography* (Ibers and Hamilton, 1974). The final calculations using anisotropic diplacement parameters converged at R1 = 0.026 for 1113 independent reflections with $I > 2\sigma(I)$. The largest shift in the final cycle was < 0.001. The resulting fractional atomic coordinates, equivalent isotropic and anisotropic displacement parameters, as well as selected interatomic distances and angles are given in Tables 2 - 4. Drawings of structural details were prepared using the program ATOMS (Dowty, 2000).

Tables 2-4

The ^{29}Si MASNMR spectra of the powdered crystals were recorded on a BRUKER Avance 500WB spectrometer operating at 99.36 MHz. A 4 mm MAS probe allowing stable spinning speeds of up to 15 kHz for several days was used. Since we obtained practically no signal after several hundred scans under the conditions used by Heidemann *et al*. (1992) in a recent NMR study of sodium

Post-print version

disilicates (π/4 pulses of 2 μs and a repetition time of 10 s), we performed a series of measurements with π/4 pulses and repetition times of between 60 s and 1800 s (at least 48 scans). From the dependence of the normalised intensity on the repetition time we estimated the longitudinal relaxation time T_1 to be of the order of 3000 s for all the silicon sites. Hence, the optimum flip-angle to maximise the signal intensity for a repetition time of 900 s is about π/4. These parameters were applied for the measurements at different MAS frequencies. The chemical shifts were referenced to neat TMS in a separate rotor.

Description of the structure

The structure of C-$Na_2Si_2O_5$ consists of a sequence of layers of tetrahedra perpendicular to *b*. A single layer can be described as being built by condensation of unbranched zweier single chains running parallel *a* or vierer single chains parallel *c* via common corners. Furthermore, each single tetrahedral sheet consists of elliptically distorted rings composed of six [SiO_4]-tetrahedra in chair conformation. The sequence of directedness for the up (U) and down (D) pointing tetrahedra within a single six-membered ring (S6R) is UDUDUD. The unit cell contains four layers of tetrahedra; a projection parallel *b* of a single sheet in the unit cell of C-$Na_2Si_2O_5$ is given in Figure 1(a). The spread in the individual Si-O bond lengths follows the trend usually observed in silicate structures: the bond distances between Si and the terminal oxygens (O(2), O(6), O(9), O(10)) are considerably shorter than the bonds to bridging oxygen atoms. The values for $\langle Si\text{-}O\rangle_{term.}$ = 1.576 Å and $\langle Si\text{-}O\rangle_{brid.}$ = 1.640 Å are in good agreement with those observed in the α -, β - and δ- modifications of $Na_2Si_2O_5$. Mean Si-O distances of the four tetrahedra given in Table 4 compare well with the value of 1.617(6) given by Baur (1978) as a mean Si-O distance in phyllosilicates. While the average

Figure 1

Post-print version

values of the O-Si-O angles for the four symmetrically independent tetrahedra are very close to the ideal value of 109.47°, the individual O-Si-O angles range from 104.8 to 115.0° for the SiO_4 groups. This suggests that the distortion of polyhedra is not very pronounced. According to Robinson *et al*. (1971) the distortion can be expressed numerically by means of the quadratic elongation (Q.E.) and the angle variance (A.V.). The values of these parameters for the different tetrahedra are listed in Table 4. The Si-O-Si angles at the bridging oxygen atoms vary between 134.4 and 137.3°. Similar values have been observed for β-$Na_2Si_2O_5$: 135.1 – 136.5° (Pant, 1968), whereas the corresponding values for the second known high-pressure modification ε- $Na_2Si_2O_5$ are considerably smaller: 127.0° - 129.3° (Fleet and Henderson, 1995).

Linkage between the layers is provided by sodium cations. They reside between the sheets in about 1.6 Å wide slabs containing either Na(1) and Na(4) or Na(2) and Na(3), respectively. Within a single slab the Na cations are located in rows running parallel *a*. Na(1) and Na(3) are surrounded by five oxygen atoms at distances varying between 2.30 and 2.58 Å. Na(2) is coordinated to six oxygen anions. The Na(4) site shows a (5+1) coordination. The five inner oxygen neighbors have bond distances between 2.30 Å and 2.58 Å. Extending the limit for coordinating anions up to 3.0 Å, an additional sixth ligand at about 2.98 Å can be found. Since typical Na-O bond lengths average about 2.44 Å (Wilson 1995) the sixth Na(4)-O distance represents a weak bond. Coordination polyhedra around the sodium cations can be described as distorted trigonal bipyramids and distorted octahedra, respectively. (cf. Figure 2).

Figure 2

Bond valence sums (BVS) for the cations were calculated using the parameterization for the Si-O and the Na-O bond given by Brown and Altermatt

Post-print version

(1985). The results range from 4.16 v.u. - 4.22 v.u. for Si and 0.87 v.u. - 1.04 v.u. for Na, close to the expected values of 4 v.u. for Si and 1 v.u. for Na, respectively. The BVS values for the oxygen anions vary between 1.91 v.u. for O(2) and 2.17 v.u. for O(7).

Results and Discussion

Comparison with β-$Na_2Si_2O_5$

A common feature of almost all structurally characterized sodium disilicates are tetrahedral layers of six-membered rings formed by the condensation of zweier single chains. The translation periods along the chains is reflected in a short lattice constant of about 4.8 - 4.9 Å (see Kahlenberg, 1999 and references cited in there). Comparing the shape of the S6R's, C- $Na_2Si_2O_5$ is closely related to β-$Na_2Si_2O_5$ (cf. Figure 1(a) and 1(b)). In both structures the rings exhibit an elliptically distortion, whereas the rings in α- and δ-$Na_2Si_2O_5$ have a ditrigonal form. The close relationship in the ring geometry is also responsible for the similar Si-O-Si angles mentioned above. However, the relationships between C- and β-$Na_2Si_2O_5$ are not limited to the geometry and the conformation of the single layers. As can be seen from Figures 3(a) and (b) in both structures identical blocks containing two layers A and B can be identified, which are related by inversion centers. Furthermore, the number of oxygen ligands of the two different Na-atoms residing between the layers A and B are identical : five and six, respectively. A detailed comparison between the individual Na-O bond distances of the corresponding sodium atoms reveals, that there exists an almost one-to-one correspondence of the Na(2) and Na(3) atoms in phase C and the cations Na(2) and Na(1) in the β-phase. The main difference between the two modifications results from the way in which the blocks are stacked. In contrast to β-$Na_2Si_2O_5$,

Post-print version

where two adjacent blocks are translationally equivalent (resulting in a two layer stacking sequence), two neighboring blocks I and II in C-$Na_2Si_2O_5$ are related by the *c*-glide planes at y = ¼ and y = ¾, respectively. Therefore, a four layer stacking sequence is observed in this phase and the sodium atoms Na(1) and Na(4) at the interface between the blocks show a different coordination environment compared to Na(2) and Na(3). Whereas the 2_1-screw axes in β-$Na_2Si_2O_5$ are located within the single layers, running parallel to the zweier single chains, the corresponding symmetry elements in phase C are oriented perpendicular to the layers.

Figure 3

Twinning

Twinning by pseudo-merohedry is a feature frequently observed in monoclinic crystals where β is close to 90°. Actually, under the petrographic microscope almost all crystals of C-$Na_2Si_2O_5$ showed a polysynthetic twinning with composition planes parallel to (001). The twinning observed on a macroscopic scale may be microscopically rationalized by the existence of domains related by twofold axes running parallel [100] or mirror planes perpendicular to [001]. The resulting two types of twin individuals and the hypothetical twin boundary within a single layer for a twinning according to $2_{[100]}$ are shown in Figure 4. At the interfaces between the domains ditrigonally shaped, six-membered rings in UDUDUD conformation are formed. Twinning according to $m_{[001]}$ also results in rings of ditrigonal shape at the domain boundary. However, the conformation of these rings would be UUDUDD. Since twinning by $2_{[100]}$ is not involved with a change the of sequence of directedness across the twin boundary this twinning model seems to be more appropriate.

Figure 4

^{29}Si MAS-NMR

Post-print version

The ^{29}Si MASNMR spectrum in Figure 5 shows four well-resolved lines with chemical shifts in the range between -86.0 ppm and -88.2 ppm. It can be fitted nicely using four Lorentzians with linewidths of 21 Hz and 24 Hz for the two low-field and the two high-field lines, respectively.

The relative intensities thus obtained are 1 : 0.99 : 0.92 : 0.89. The small deviations from unity could easily be caused by the individual relaxation times in the various sites differing by not more than 10% from each other (cf. Experimental). The chemical shifts fall in the range observed for Q^3 groups in other alkali disilicates (Heidemann *et al*. 1992, de Jong *et al*. 1998). The signal-to-noise ratio is sufficient to rule out any significant contributions from amorphous by-products.

Figure 5

Although there was not quite enough sample to fill the 4 mm rotor we attempted to determine the parameters describing the anisotropy of the chemical shift (CSA), *i. e*. the anisotropy Δ and the asymmetry η. These parameters contain valuable information on the local geometry of different silicon sites (Grimmer 1993). The ^{29}Si MASNMR spectrum obtained at an MAS frequency of 2.2 kHz is given in Figure 6. The spectral range in which the five spinning sidebands are observed indicates anisotropy values characteristic of Q^3 units (Heidemann *et al*. 1992, Grimmer 1993). However, the signal-to-noise ratio achieved is too low for a reliable determination of the CSA parameters, in particular, to ascertain any subtle differences between the non-equivalent sites. To obtain an adequate signal-to-noise ratio in a reasonable time, the measurements have to be repeated with a larger amount of sample using a 7 mm rotor.

Figure 6

The four well-resolved lines in the ^{29}Si MASNMR spectrum (Figure 5)

Post-print version

undoubtedly have to be attributed to the presence of the four non-equivalent sites. However, their actual assignment to the individual sites turns out to be a problem. Generally, the chemical shift-structure correlation is the main reason why the combination of X-ray diffraction with solid-state NMR spectroscopy is so efficient. The close correlation between ^{29}Si NMR chemical shift and geometrical properties such as Si-O bond lengths and Si-O-Si bond angles α was recognized soon after the first paper on the application of ^{29}Si MASNMR to silicates (Lippmaa *et al*. 1980) was published. Basic concepts and the early work on the theoretical interpretation of ^{29}Si NMR chemical shifts in zeolites and other silicates and quantitative correlations between chemical shift and structure parameters has been reviewed by Engelhardt and Michel (1987).

We have applied several correlation equations established for Q^3 units using either the Si-O bond lengths or the bond angles α. The results thus obtained are inconsistent with each other (see Table 5). The equations based on the Si-O distances predict a much wider range of chemical shifts than actually observed in the spectrum while those based on the bond angles predict a significantly narrower one than is observed. Furthermore, the two types of correlations suggest completely different sequences of the lines: From the bond-angle based correlations the order Si(3), Si(2), Si(1), and Si(4) (from low to high field) is obtained, whereas the Si-O distance based correlations produce the opposite sequence. Heidemann *et al*. (1992) have reported the similar discrepancy for β–$Na_2Si_2O_5$.

Table 5

Using different siliceous zeolites for which high-quality structure data were available, Fyfe *et al*. (1993) have critically evaluated several chemical shift-structure correlations for Q^4 units. Both the mean Si-Si distance, that is, the

Post-print version

distance between the target silicon atom and its first nearest neighboring silicon atoms, and the mean value of the cos α / (cos α-1) function were found to have a linear relationship with the isotropic ^{29}Si NMR chemical shift with very high correlation coefficients. The main limitation in the structure-chemical shift correlations is the accuracy of the X-ray data, particularly when refinements of powder data are involved. Errors of 0.001 Å in the Si-O bond lengths (Grimmer and Radeglia 1984, Engelhardt and Michel 1987, Grimmer 1993), 0.01 Å in the Si-Si distances (Fyfe *et al*. 1993) or 2° in the mean bond angles (Engelhardt and Radeglia 1984, Engelhardt and Michel 1987) correspond to comparatively large shift uncertainties of the order of 1 ppm. Very recently, Hochgräfe *et al*. (2000) have demonstrated that improved structural data can be obtained from lattice energy minimization calculations compared to those from Rietveld analysis, provided that the topology of the framework is known. These authors pointed out that they used Si-Si distances since the true crystallographic Si-O distances are often obscured by static or dynamic disorder of the oxygen atoms, whereas a similar disorder has never been observed for silicon atoms in zeolite framework structures. Hence, the use of geometry data that do not depend on oxygen positions might be superior even if single-crystal data are available.

To the best of our knowledge, no quantitative correlation based on Si-Si distances has been established for Q^3 units. Assuming the same slope of the chemical shift *versus* mean Si-Si distance correlation (about -115 ppm/Å) as obtained for Q^4 units by Fyfe *et al*. (1993), the difference of 0.015 Å between the mean Si-Si distances for Si(3) and Si(4) in the silicate under study corresponds to a chemical shift difference of 1.7 ppm. This value fits the experimentally observed shift difference of 2.2 ppm of the most separated lines (Figure 5) much better than the

Post-print version

rather large differences derived from the Si-O bond lengths or the rather small ones derived from the Si-O-Si bond angles. Since the above given slope is negative, the resonance line at the lowest field should be assigned to Si(3) and that at the highest field to Si(4), giving the same sequence as the correlations based on the bond angles (cf. Table 5). However, this argument is rather tentative and further work is necessary to put the assignment on a firm footing. Considering the great similarity of the environments of the four silicon sites it might be a difficult problem to solve.

Acknowledgement

Financial support for this work has been received from the Deutsche Forschungsgemeinschaft under the grant Ka1342/1. The help of Prof. D. Lindsley (SUNY at Stony Brook) during the hydrothermal experiments is gratefully acknowledged. Furhermore, the authors would like to thank Dr. A.-R. Grimmer (Berlin) for helpful comments with regard to the applicability of the different chemical shift-structure correlations.

Post-print version

References

Altomare A, Cascarano G, Giacovazzo C, Guagliardi A, Burla MC, Polidori G, Camalli M (1992) SIR92 – a program for automatic solution of structures by direct methods. J Appl Cryst 27:435

Baur WH (1978) Variation of mean Si-O bond lengths in silicon-oxygen tetrahedra. Acta Cryst B34:1751-1756

Brown ID, Altermatt D (1985) Bond-valence parameters obtained from a systematic analysis of the Inorganic Crystal Structure Database. Acta Cryst B41:244-247

de Jong BHWS, Super HTJ, Spek AL, Veldman N, Nachtegaal G, Fischer JC (1998) Mixed alkali systems: Structure and ^{29}Si MAS NMR of $Li_2Si_2O_5$ and $K_2Si_2O_5$. Acta Cryst B54:568-577

Dowty E. (2000) ATOMS, Version5.1 - Shape Software.

Engelhardt G, Radeglia R (1984) A semi-empirical quantum-chemical rationalization of the correlation between SiOSi angles and ^{29}Si NMR chemical shifts of silica polymorphs and framework aluminosilicates (zeolites). Chem Phys Lett 108:271-274

Engelhardt G, Michel D (1987) High-resolution solid state NMR of silicates and zeolites. Wiley, Chichester, pp 122-134

Post-print version

Fleet ME, Henderson GS (1995) Epsilon sodium disilicate: a high-pressure layer structure [$Na_2Si_2O_5$]. J Sol State Chem 119:400-404

Grimmer A-R, Radeglia R (1984) Correlation between the isotropic Si-29 chemical shifts and the mean silicon-oxygen bond length in silicates. Chem Phys Lett 106:262-265

Grimmer A-R (1993) Shielding tensor data and structure: the bond-related chemical shift concept. In: Tossell JA (ed) Nuclear magnetic shieldings and molecular structure. Kluwer, Dordrecht, pp 191-201

Heidemann D, Hübert C, Schwieger W, Grabner P, Bergk KH, Sarv P (1992) ^{29}Si- und ^{23}Na-Festkörper-MAS-NMR-Untersuchungen an Modifikationen des $Na_2Si_2O_5$. Z Anorg Allg Chem 617:169-177

Hochgräfe M, Gies H, Fyfe CA, Feng Y, Grondey H (2000) Lattice energy-minimization calculation in the further investigation of XRD and NMR studies of zeolite frameworks. Chem Mater 12:336-342

Hoffmann W, Scheel HJ (1969) Über die γ - und δ - Modifikationen des Natriumdisilikates, $Na_2Si_2O_5$. Z Kristallogr 129:396-404

Ibers JA, Hamilton WC, Eds. (1974) International tables for X - ray crystallography, Volume IV, Kynock, Birmingham, U.K.

Post-print version

Jacobsen, H (1991) Neue Untersuchungen an Natriumdisilikat ($Na_2Si_2O_5$). Diplomarbeit, Universität Hannover.

Janes N, Oldfield E (1985) Prediction of silicon-29 nuclear magnetic resonance chemical shifts using a group electronegativity approach: application to silicate and aluminosilicate structures. J Am Chem Soc 107:6769-6775

Kahlenberg V, Dörsam G, Wendschuh-Josties M, Fischer RX (1999) The crystal structure of δ-$Na_2Si_2O_5$. J Sol State Chem 146:380-386

Kanzaki M, Xue X, Stebbins JF (1998) Phase relations in Na_2O-SiO_2 and $K_2Si_4O_9$ systems up to 14 GPa and ^{29}Si NMR study of the new high-pressure phases: implications to the structure of high-pressure silicate glasses. Phys Earth Planet Int 107:9-21

Lippmaa E, Mägi M, Samoson A, Engelhardt G, Grimmer A-R (1980) Structural studies of silicates by solid-state high-resolution ^{29}Si NMR. J Am Chem Soc 102:4889-4893

Maekawa H, Yokokawa T (1997) Effects of temperature on silicate melt structure: A high temperature Si-29 NMR study of $Na_2Si_2O_5$. Geochim Cosmochim Acta 61:2569-2575

Pant AK (1968) A reconsideration of the crystal structure of β-$Na_2Si_2O_5$. Acta Cryst B24:1077-1083

Post-print version

Rieck HP (1996) Natriumschichtsilicate und Schichtkieselsäuren. Nachr Chem Tech Lab 44:699-704

Robinson K, Gibbs GV, Ribbe PH (1971) Quadratic elongation : A quantitative measure of distortion in coordination polyhedra. Science 172:567-570

Sheldrick, GM (1993) SHELXL-93. Program for the refinement of crystal structures. Universität Göttingen, Germany.

Smith KA, Kirkpatrick RJ, Oldfield E, Henderson DM (1983) High resolution silicon-29 nuclear magnetic resonance spectroscopic study of rock-forming silicates. Am Mineral 69:1206-1215

Willgallis A, Range KJ (1963) Zur Polymorphie des $Na_2Si_2O_5$. Glastechn Ber 37: 194-200

Williamson J, Glasser FP (1966) The crystallisation of $Na_2O \cdot 2SiO_2$ - SiO_2 glasses. Phys Chem Glasses 7:127-138

Wilson, AJC, Ed. (1995) International Tables for Crystallography, Volume C, Mathematical, Physical and Chemical Tables, Kluwer, Dordrecht.

Wolf F, Schwieger W (1979) Zum Ionenaustausch einwertiger Kationen an synthetischen Natriumpolysilicaten mit Schichtstruktur. Z Anorg Allg Chem 457:224-228.

Post-print version

Figure captions

Figure 1. Single layer of tetrahedra in (a) C-$Na_2Si_2O_5$ and (b) β- $Na_2Si_2O_5$. The numbers within the tetrahedra of phase C correspond to the labels of the central Si atoms in Table 2.

Figure 2. The two principally different coordination polyhedra for Na observed in C-$Na_2Si_2O_5$: (a) distorted trigonal bipyramids (shown for Na(3) as an example) and (b) distorted octahedra (for Na(2)).

Figure 3. Stacking sequences of the layers in (a) C-$Na_2Si_2O_5$ and (b) β- $Na_2Si_2O_5$. Dark grey circles correspond to the Na-atoms linking the sheets. The labeling of the sodium cations in the β-phase follows the choice of Pant (1968)

Figure 4. Possible twinning model for C-$Na_2Si_2O_5$ with $2_{[100]}$ selected as the twin element.

Figure 5. ^{29}Si MASNMR spectrum of C-$Na_2Si_2O_5$ recorded at an MAS frequency of 12 kHz (232 scans, π/4 pulses, repetition time: 900 s, cf. Experimental).

Figure 6. ^{29}Si MASNMR spectrum of C-$Na_2Si_2O_5$ recorded at an MAS frequency of 2.2 kHz (360 scans, π/4 pulses, repetition time: 900 s, cf. Experimental).

Post-print version

Table 1. Data collection and refinement parameters

(A)	Crystal data	
	a (Å)	4.8521(4)
	b (Å)	23.9793(16)
	c (Å)	8.1410(6)
	β (°)	90.15(1)
	V ($Å^3$)	947.2(2)
	Space group	$P\,2_1/c$
	Z	8
	Chemical formula	$Na_2Si_2O_5$
	D_{calc} (g cm^{-3})	2.56
	μ (mm^{-1})	0.86
(B)	Intensity measurements	
	Crystal shape	Plate
	Diffractometer	Stoe – IPDS
	Monochromator	Graphite
	Radiation	Mo-K_α, λ = 0.71073 Å
	X-ray power	50 kV, 40 mA
	Detector to sample distance	80 mm
	Rotation width in ϕ (°)	1.0
	No. of exposures	200
	Irridation time / exposure (min.)	5.00
	θ - range (°)	1.45° - 24.2°
	Reflection range	$\lvert h \rvert \leq 5$; $\lvert k \rvert \leq 27$; $\lvert l \rvert \leq 9$
	No. of measured reflections	6124

Post-print version

	No. of unique reflections in 2/m	1495
	R_{int} in 2/m after absorption correction	0.0354
	No. of observed reflections ($I > 2\ \sigma(I)$)	1113
(C)	Refinement of the structure	
	No. of parameters used in the refinement	163
	R1 ($F_o > 4\ \sigma(F_o)$) ; R1 (all data)	0.0261 ; 0.0391
	wR2 ($F_o > 4\ \sigma(F_o)$)	0.0658
	Weighting parameter a	0.0427
	Goodness of Fit	0.931
	Final $\Delta\rho_{min}$ (e / $Å^3$)	-0.26
	Final $\Delta\rho_{max}$ (e / $Å^3$)	0.39
	$R1 = \Sigma \ \|\|F_o\| - \|F_c\|\| / \ \Sigma \ \|F_o\|$	$wR2 = (\Sigma(w(F_o^2 - F_c^2)^2) / \Sigma(w(F_o^2)^2))^{½}$
	$w = 1 / (\sigma^2 (F_o^2) + (aP)^2)$	$P = (2F_c^2 + \max(F_o^2,0)) / 3$

Post-print version

Table 2. Atomic coordinates and equivalent isotropic displacement factors. U_{eq} is defined as one third of the trace of the orthogonalized U_{ij} tensor. All atoms occupy general positions.

Atom	x	y	z	U_{eq}
Si(1)	0.2961(2)	0.36325(4)	0.1966(1)	0.0146(2)
Si(2)	0.6843(2)	0.34077(4)	0.6429(1)	0.0145(2)
Si(3)	0.1831(2)	0.40821(4)	0.5373(1)	0.0145(2)
Si(4)	0.7948(2)	0.38941(4)	-0.0185(1)	0.0152(2)
Na(1)	0.2299(3)	0.26138(6)	0.5247(2)	0.0244(3)
Na(2)	0.2743(3)	0.51408(5)	0.3548(2)	0.0215(3)
Na(3)	0.2534(3)	0.47281(5)	-0.1019(2)	0.0225(3)
Na(4)	0.7548(3)	0.28108(5)	0.2783(2)	0.0229(4)
O(1)	0.1210(4)	0.3844(1)	0.0352(3)	0.0195(5)
O(2)	0.2339(4)	0.3015(1)	0.2523(3)	0.0199(6)
O(3)	0.6209(4)	0.3690(1)	0.1429(3)	0.0184(5)
O(4)	0.2440(4)	0.4105(1)	0.3392(3)	0.0182(5)
O(5)	0.7431(4)	0.3414(1)	-0.1590(3)	0.0192(5)
O(6)	0.7456(4)	0.2819(1)	0.5655(3)	0.0184(5)
O(7)	0.3573(4)	0.3561(1)	0.6162(3)	0.0182(5)
O(8)	-0.1423(4)	0.3920(1)	0.5597(3)	0.0180(5)
O(9)	0.2452(4)	0.4667(1)	0.6166(3)	0.0183(5)
O(10)	0.7336(4)	0.4511(1)	-0.0767(3)	0.0195(5)

Post-print version

Table 3. Anisotropic displacement parameters ($Å^2$). The anisotropic displacement factor exponent takes the form: $-2\pi^2 [h^2 a^{*2} U_{11} + ... + 2 h k a^* b^* U_{12}]$

Atom	U_{11}	U_{22}	U_{33}	U_{23}	U_{13}	U_{12}
Si(1)	0.0136(4)	0.0166(5)	0.0135(5)	-0.0002(4)	0.0012(3)	0.0002(4)
Si(2)	0.0134(5)	0.0156(5)	0.0145(5)	0.0000(4)	-0.0001(4)	0.0002(4)
Si(3)	0.0132(5)	0.0156(5)	0.0147(5)	0.0003(4)	0.0008(4)	0.0002(4)
Si(4)	0.0135(5)	0.0183(5)	0.0137(5)	-0.0003(4)	-0.0002(4)	-0.0001(4)
Na(1)	0.0240(8)	0.0246(7)	0.0247(8)	0.0049(6)	-0.0008(6)	-0.0009(8)
Na(2)	0.0215(7)	0.0208(7)	0.0221(8)	0.0024(6)	0.0015(6)	-0.0001(4)
Na(3)	0.0219(7)	0.0248(8)	0.0208(8)	-0.0031(6)	0.0002(6)	-0.0018(6)
Na(4)	0.0211(7)	0.0266(8)	0.0209(8)	-0.0027(6)	0.0005(6)	0.0006(6)
O(1)	0.0165(12)	0.0243(12)	0.0176(13)	0.0021(10)	0.0010(9)	-0.0006(10)
O(2)	0.0196(12)	0.0195(12)	0.0206(14)	-0.0018(10)	-0.0002(10)	-0.0007(9)
O(3)	0.0172(12)	0.0221(12)	0.0159(12)	0.0006(10)	-0.0011(9)	-0.0002(9)
O(4)	0.0204(12)	0.0182(12)	0.0159(13)	-0.0002(10)	0.0022(9)	-0.0002(9)
O(5)	0.0220(12)	0.0189(12)	0.0166(13)	0.0015(10)	-0.0006(9)	-0.0005(10)
O(6)	0.0194(12)	0.0179(12)	0.0179(14)	-0.0002(10)	0.0002(9)	0.0001(9)
O(7)	0.0160(12)	0.0187(12)	0.0199(13)	0.0020(10)	-0.0001(9)	-0.0004(9)
O(8)	0.0189(12)	0.0172(12)	0.0180(13)	0.0012(10)	0.0011(9)	0.0004(9)
O(9)	0.0196(12)	0.0203(12)	0.0149(13)	-0.0005(10)	0.0002(10)	-0.0004(10)
O(10)	0.0198(12)	0.0192(12)	0.0195(13)	-0.0006(10)	-0.0002(9)	0.0022(9)

Post-print version

Table 4. Selected bond distances (Å) and angles (deg.).

Si(1)	-O(2)	1.578(3)	Si(2)	-O(6)	1.575(3)
	-O(3)	1.642(2)		-O(8)	1.637(3)
	-O(4)	1.642(3)		-O(5)	1.637(3)
	-O(1)	1.643(3)		-O(7)	1.643(2)
Mean		1.626	Mean		1.623
Si(3)	-O(9)	1.573(3)	Si(4)	-O(10)	1.581(3)
	-O(8)	1.637(2)		-O(3)	1.638(3)
	-O(7)	1.639(3)		-O(5)	1.642(3)
	-O(4)	1.641(3)		-O(1)	1.645(2)
Mean		1.623	Mean		1.627
Na(1)	-O(2)	2.389(3)	Na(2)	-O(9)	2.387(2)
	-O(2)	2.417(3)		-O(10)	2.413(3)
	-O(6)	2.425(2)		-O(9)	2.420(3)
	-O(7)	2.468(3)		-O(8)	2.443(3)
	-O(6)	2.571(3)		-O(4)	2.491(3)
				-O(9)	2.574(2)
Na(3)	-O(9)	2.297(3)	Na(4)	-O(6)	2.299(3)
	-O(10)	2.334(3)		-O(6)	2.339(3)
	-O(10)	2.396(3)		-O(2)	2.386(2)
	-O(1)	2.481(3)		-O(3)	2.465(3)
	-O(10)	2.584(2)		-O(2)	2.583(2)
				-O(5)	2.982(3)

Post-print version

O – T – O angles

O(2)-Si(1)-O(4)	114.48(13)	O(6)-Si(2)-O(8)	114.17(13)
O(3)-Si(1)-O(2)	109.86(12)	O(5)-Si(2)-O(6)	111.71(13)
O(3)-Si(1)-O(4)	106.25(12)	O(5)-Si(2)-O(8)	108.20(13)
O(1)-Si(1)-O(2)	114.87(13)	O(7)-Si(2)-O(6)	109.34(12)
O(1)-Si(1)-O(4)	105.79(13)	O(7)-Si(2)-O(8)	105.94(12)
O(1)-Si(1)-O(3)	104.82(12)	O(7)-Si(2)-O(5)	107.10(12)
Mean	109.35	Mean	109.41
O(8)-Si(3)-O(9)	110.48(12)	O(3)-Si(4)-O(10)	115.03(13)
O(7)-Si(3)-O(9)	114.90(13)	O(5)-Si(4)-O(10)	114.77(13)
O(7)-Si(3)-O(8)	105.78(12)	O(5)-Si(4)-O(3)	105.74(13)
O(4)-Si(3)-O(9)	109.80(13)	O(1)-Si(4)-O(10)	109.13(12)
O(4)-Si(3)-O(8)	107.08(12)	O(1)-Si(4)-O(3)	105.20(12)
O(4)-Si(3)-O(7)	108.46(13)	O(1)-Si(4)-O(5)	106.20(12)
Mean	109.42	Mean	109.35

T – O – T angles

Si(3)-O(8)-Si(2)	136.18(15)
Si(4)-O(1)-Si(1)	136.89(15)
Si(2)-O(7)-Si(3)	136.02(15)
Si(1)-O(3)-Si(4)	137.32(15)
Si(4)-O(5)-Si(2)	135.95(16)
Si(1)-O(4)-Si(3)	134.43(16)

Post-print version

Table 5 Compilation of geometry data of the silicon sites and calculated isotropic chemical shifts using established empirical correlations

Parameter	Si(1)	Si(2)	Si(3)	Si(4)
<d(Si-O)> (Å)	1.6263	1.6230	1.6225	1.6265
$\sum$(EN)[a]	15.1974	15.1938	15.1827	15.2085
<∠Si-O-Si> (°)	136.21	136.05	135.54	136.72
<d(Si-Si)> (Å)	3.047	3.040	3.036	3.051
δ_{iso} = 844.2 <d(Si-O)>/Å - 1459.5 (ppm) (Smith *et al*. 1983)	-86.58	-89.36	-89.79	-86.41
δ_{iso} = 1187 <d(Si-O)>/Å - 2014 (ppm) (Grimmer and Radeglia 1984)	-83.58	-87.50	-88.09	-83.34
δ_{iso} = -24.336 $\sum$(EN) + 279.27 (ppm) (Janes and Oldfield 1985)	-90.57	-90.49	-90.22	-90.84
δ_{iso} = -0.725 <∠Si-O-Si> + 9.054 (ppm) (de Jong *et al*. 1998)	-89.70	-89.58	-89.21	-90.07

[a] Sum of bond electronegativities calculated according to Janes and Oldfield (1985): EN(Si-O) = ∠Si-O-Si / 136.79° + 2.9235 and EN(O-Na) = 3.4395.

Post-print version

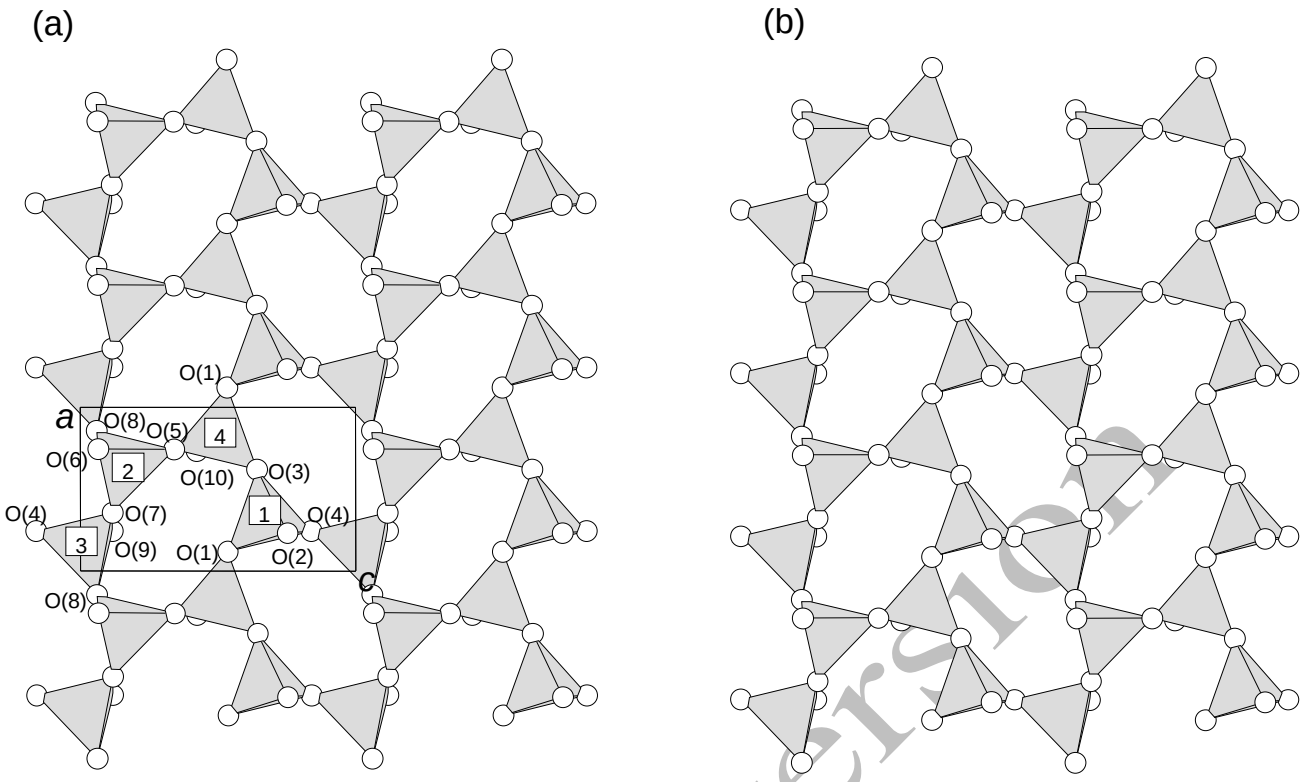

Fig. 1

Post-print version

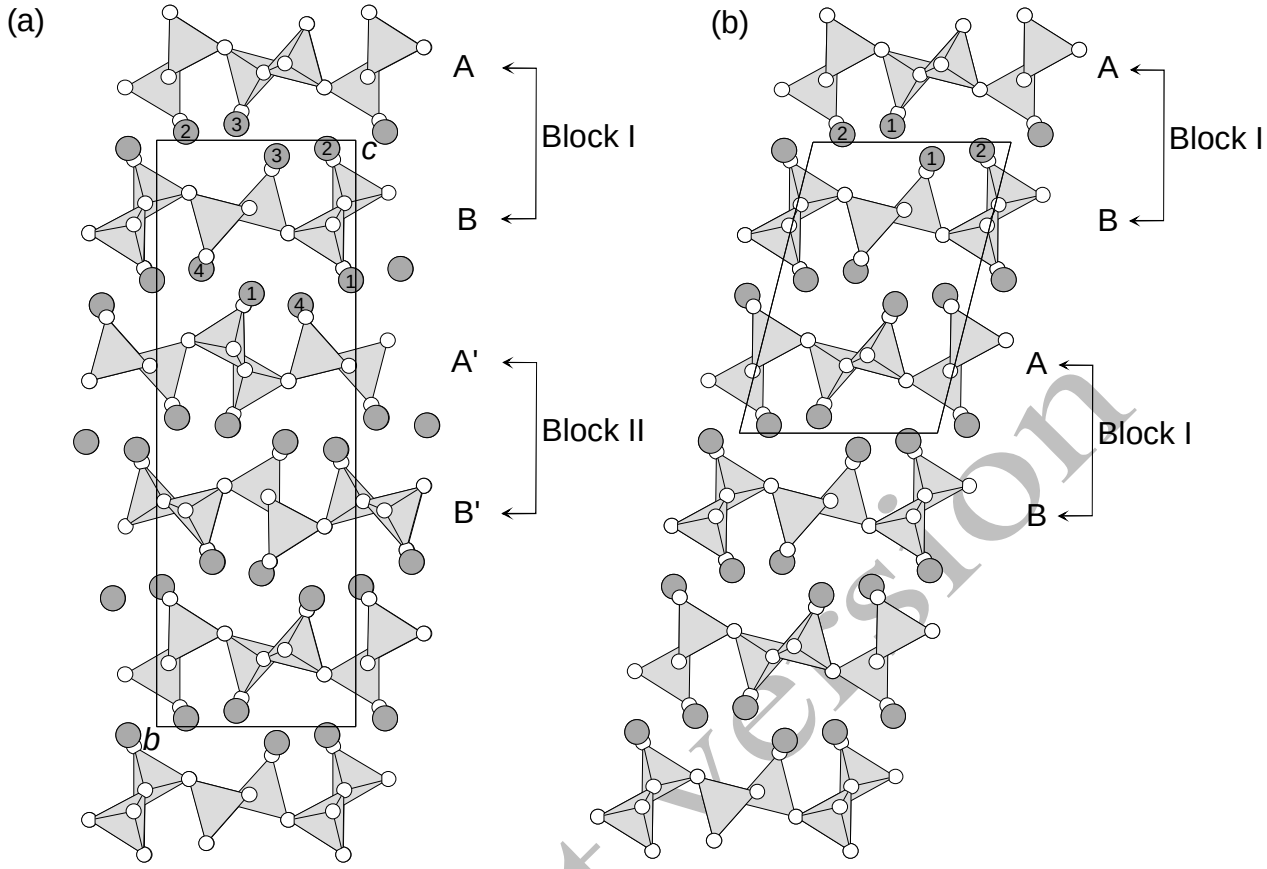

Fig. 3

Post-print version

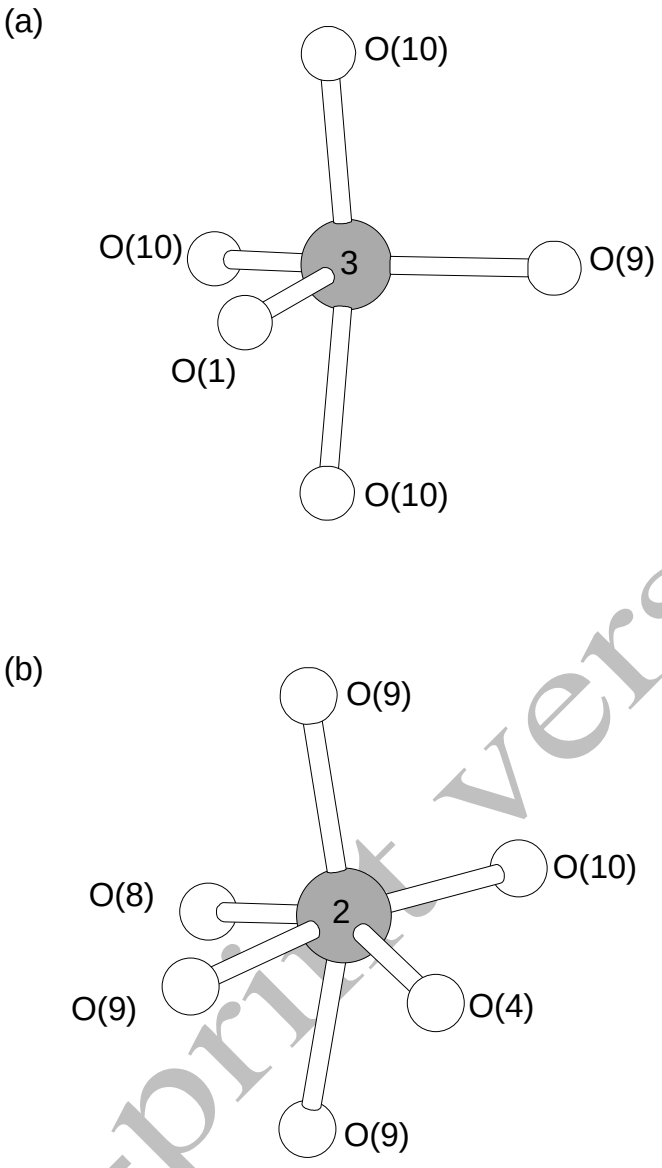

Fig. 2

Post-print version

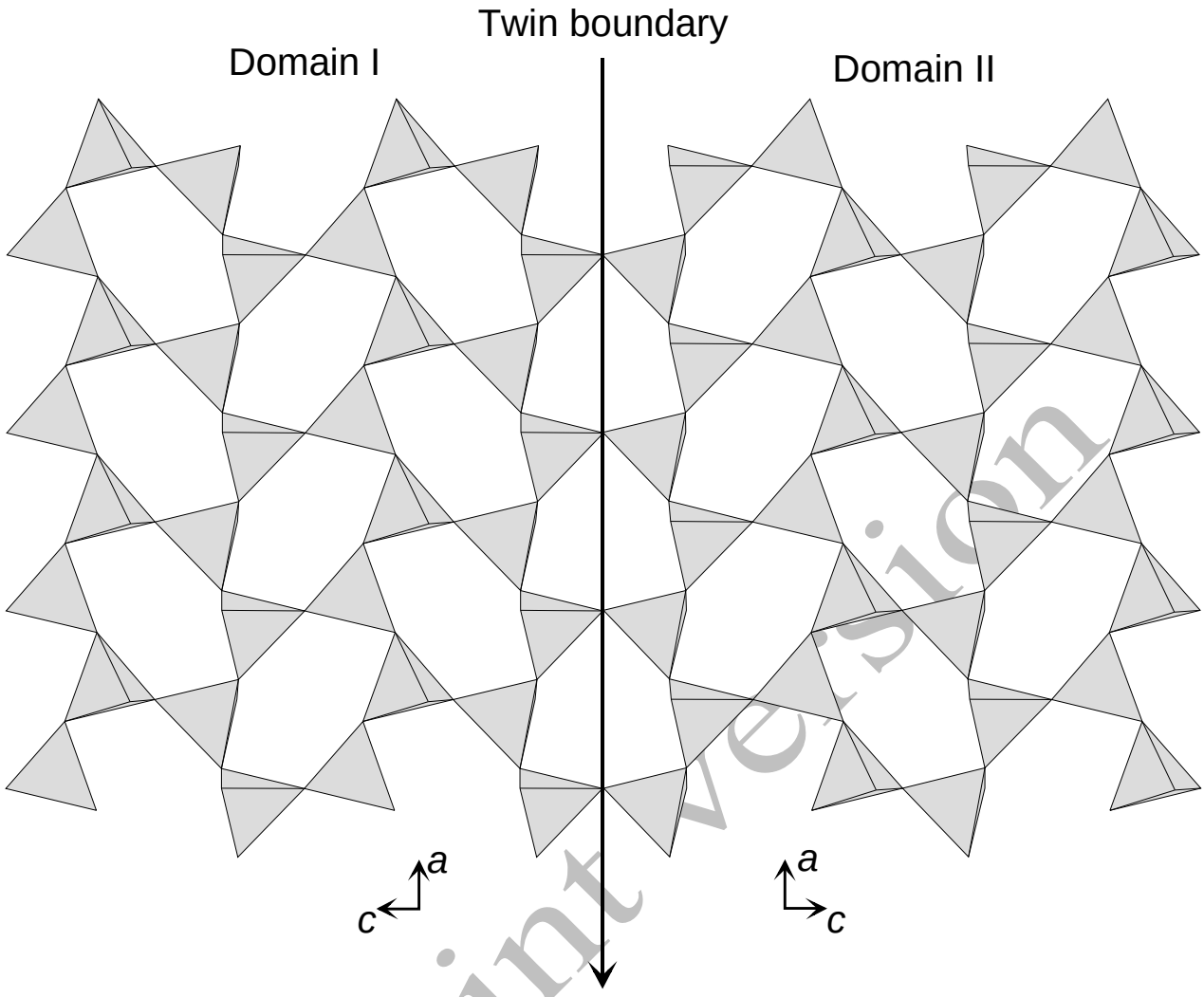

Fig. 4

Post-print version

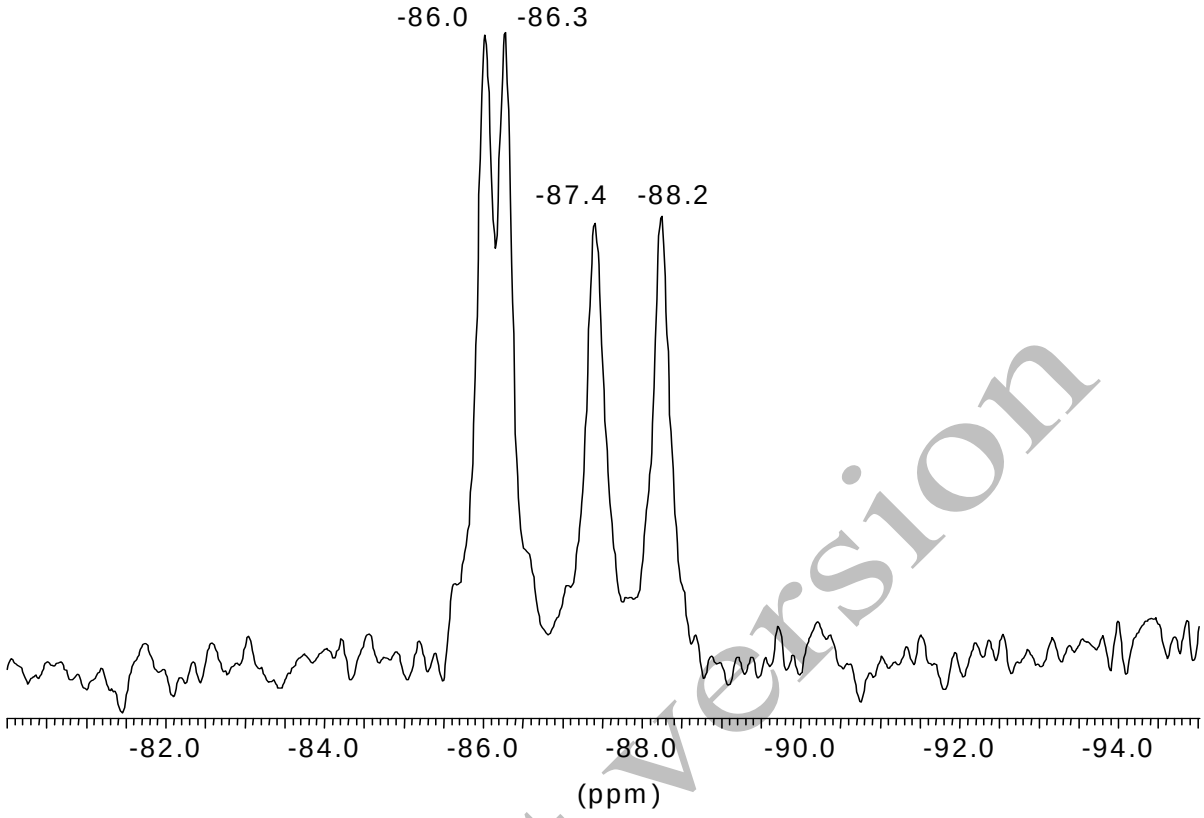

Fig. 5

Post-print version

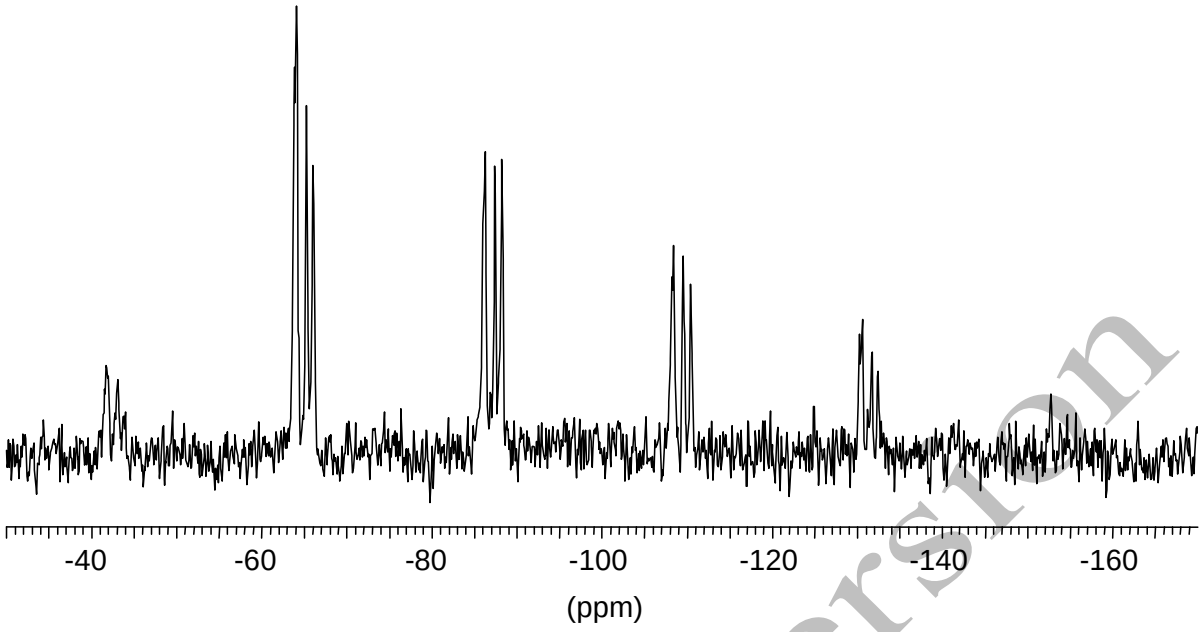

Fig. 6

Post-print version